Civil and Sustainable Urban Engineering

Research Article
Volume 1(1), 2021, 50-59
https://doi.org/10.53623/csue.v1i1.38

Analysis of Rectangular Reinforced Concrete Liquied Tanks by Using Yield Line Theory

Yousef Zandi , Afram Keivani*

Department of Engineering, Faculty of Civil Engineering, Tabriz Branch, Islamic Azad University, Tabriz, Iran.

* Correspondence: keivani@iaut.ac.ir

SUBMITTED: 25 October 2021; REVISED: 11 November 2021; ACCEPTED: 12 November 2021

ABSTRACT: In the analysis of rectangular reinforced liquid storage tanks, a method assuming linear-elastic behavior for material can be used, i.e., the strip method, the moment coefficient method, the finite element method, etc. In the analysis of these types of tanks, tank walls can be considered as slabs. In this study, tank walls were analyzed as slabs subjected to hydrostatic loading; in the analysis, the yield line theory is used because it is more suitable for the linear inelastic behavior of reinforced concrete slabs than the ones based on the linear elastic theory. An iterative algorithm based on yield line theory is presented for the design of isotropically reinforced rectangular concrete slabs supported along all four edges. A computer program is coded which predicts the location of yield lines for the slabs depending upon certain parameters. As a result of this prediction, the manual design of such slabs can be significantly simplified by the use of the coefficient obtained by using the program. It was shown that the analytical computation of the ultimate moment per unit length requires the solution of a highly nonlinear system of equations. This difficulty was overcome by utilizing an iterative technique within the computer program. It also gives the value of the ultimate moment per unit length of the yield line.

KEYWORDS: Liquid tanks; reinforecd concrete; reinforced slads; yield line

1. Introduction

The methods based on yield line theory were more suitable for the design of reinforced concrete slabs than the other methods based on linear elastic theory—the strip method, the moment coefficient method, etc.—because they consider the realistic behavior of such elements. The behavior of these slabs consists of four stages under increasing loads and can be listed as elastic, cracking, plastic, and collapse. In the initial stage, the distribution of bending moments corresponds to the elastic bending moment diagram. When the first crack takes place, the second moment of area of the section reduces, and this reduction causes a redistribution of the bending moment diagram. In the plastic stage, for an under-reinforced section, rebars start to yield as loading increases. This results in spreads along the section where most of the cracks concentrate. These failure lines are known as yield lines. At the final stage, the failure lines spread along the slab and transform it into a collapse mechanism following an infinitesimal

increase in the loads. At this stage, the failure occurs by crushing the concrete in the compression zone [1-10].

In this study, a computer program was presented based on an iterative algorithm. The algorithm uses the yield line theory and obtains the ultimate moment per unit length of an isotropically reinforced slab that was subjected to hydrostatic pressure loading. The program also predicts the location of yield lines for slabs supported along all four edges. As a result, the manual design of such slabs can be significantly simplified by the use of a coefficient obtained by using the program.

2. Yield Line Theory

2.1. Basic assumptions

The yield line theory assumes the concrete slab was a rigid plastic material. As a result of this assumption, elastic deformations at the collapse were ignored [11–14]. In addition, at collapse, the slab was considered to be separated into a number of parts by yield lines, each a rigid element. This reduces the deformation to rotations of these parts depending on the boundary conditions of the slab. The deformed shape of the slab at collapse has multiple faces.

Yield line theory applies kinematic theory to reinforced concrete supporting members. Therefore, according to kinematic theory, the ultimate failure load of a slab was either equal to or smaller than its experimental failure load. If the kinematic mechanism used was the collapse mechanism, and if it was possible to have an acceptable moment distribution, the ultimate load computed for any assumed collapse mechanism was the closest load to the experimental collapse load. In order to be sure that this condition was satisfied, and in cases where experimental verification was not possible, it was necessary to determine a statically acceptable moment distribution that gives the same failure load for the slab considered. In other words, the uniqueness theorem was used to obtain the closest load to the experimental collapse load. Experimental studies conducted thus far show that the results obtained using Johansen criteria were more conservative than experimental results [4, 7, 10, 12, 15, 18].

2.2. Application

The yield line theory was applied in two stages. In the first stage, different possible collapse mechanisms were defined depending on the support conditions and loading of the slab. In the second stage, the predetermined collapse mechanism with the smallest collapse load was found. This was carried out by using either the energy or equilibrium method.

2.2.1. Possible collapse mechanisms

Determination of the possible collapse mechanisms was carried out by applying the following theorems Johansen [18-21]:

a) The plastic hinge line between two rigid elements of the slabs passes through the intersection of the rotation axis of these elements. In the case where the slab was supported along one side, the rotation axis has to coincide with the support line as shown in Figure1. If the rotation $_i$ of the different slab parts is known, all possible collapse mechanisms can

be found by using this theorem. On the other hand, if the collapse mechanism was known, the rotation of different slab parts can be approximately predicted.

b) If the rotation axis of the different slab parts and the ratio of their rotation angles θ_i to any selected part was known, then the collapse mechanism becomes apparent. If the deformed slab was cut by a plane paralel to the plane of supports at an arbitrarily selected distance h, the intersection lines of this plane with different elements are known as contours. The distance between the contours and the rotation axis of an element is h/θ_i where h is the deflection of the plate. These contours, on the other hand, intersect the yield lines. In this case the yield lines were determined by intersecting the rotation axis with contours as shown in Figure 1.

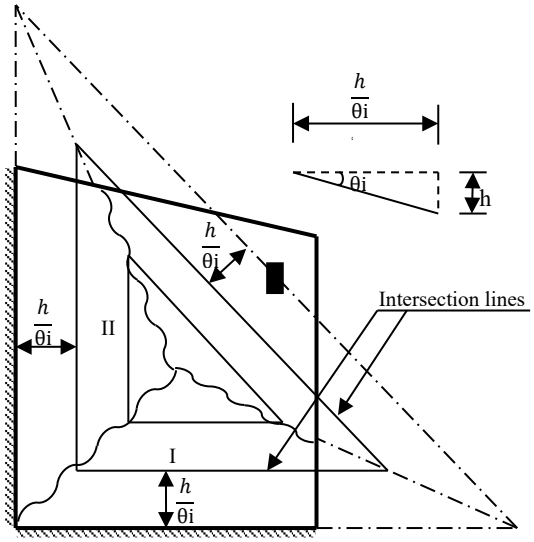

Figure 1. Determination of the possible collapse mechanisms.

2.2.2. Analysis methods

a) Virtual work method

Let the slab undergo a deflection δ which is compatible with its support conditions. Work done by external loads was equated to work done by internal forces. Since the collapse mechanism has only linear plastic hinge lines, the virtual work equation becomes:

$$\sum P_i\delta_i + P_j\delta_j dxdy = m_n \alpha ds, \quad (1)$$

where P_i is the point load and δ_i is the deflection that P_i undergoes, P_j is the uniformly distributed load, and δ_j is the deflection it causes, α is the rotation of the plastic hinge line and m_n is the bending moment on the unit length of the yield line. It was apparent that deflection δ_i and δ_j and rotation α can be related to δ. This leads having δ_i and δ_j in both sides of Eq.(1), which lead to an expression for m_n [2,5,13].

b) Equilibrium method

In the equilibrium method, equations were written for each rigid element of the collapse mechanism. For n number of rigid elements, 3n number of equilibrium equations were obtained. In the virtual work method the work done by shear forces and torsional moments along the yield line were not taken into account because their work was equal to zero. However, in the equilibrium method these internal forces, either directly or as a system of statically equivalent forces, were required to be considered in the equilibrium equations.

Solutions of the equilibrium equations gives the nodal forces and dimensional parameters of the collapse mechanism. As a result a relationship was obtained between the collapse load and the bending moment per unit lenght m [20-22]. It was apparent that the solution found will be an upper bound solution. However, it should be noted that the solution obtained using a statically acceptable moment distribution for a kinematically acceptable collapse mechanism was the closest one to the ultimate solution.

The equilibrium can either be solved by any direct method or if required an iterative approach can be employed by assuming initial values for the dimensional parameters of the slab. As a result, for each rigid slab part of the mechanism, a relationship was obtained between the loads acting and the bending moment per unit length along the yield line. By comparing the values of these moments m_1, m_2,…, m_n for each slab part, new values of these parameters were decided. This repetitive process was continued until convergence was obtained.

3. Design of Isotropically Reinforced Concrete Slabs Subjected Tohydrostatic Pressure

3.1. Algorithm

The design of reinforced concrete slabs subjected to hydrostatic loading was carried out for any support condition using Johansen's plasticity criteria [4,7,8]. In this criteria, the support conditions were taken into account by considering a parameter φ which is equal to 0 for simple supports, 1 for fixed supports and between 0 and 1 for elastic-encastre supports.

The yield line pattern of a rectangular reinforced concrete slab supported along all four edges and subjected to hydrostatic pressure is given in Figure 2. The horizontal yield line KL separates the slab into four parts. The support conditions of these slabs were all different from each other. Therefore, letting m be the ultimate moment per unit length in the slab, the support moments of these slab parts become $\varphi_1 m$, $\varphi_2 m$, $\varphi_3 m$, and $\varphi_4 m$.

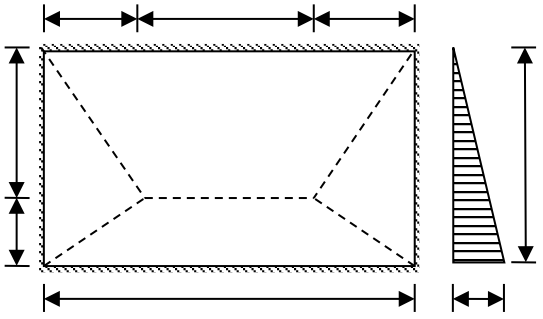

Figure 2. The yield line pattern of a rectangular slabs.

Although the yield line KL was known to be horizontal, its position was not accurately known. This was due to the fact that the position was dependent upon three unknowns α, β_1, and β_2. Since the ultimate moment per unit length m was not also known, the number of unknowns rises to four.

On the other hand, it was possible to write four equilibrium equations, with each one corresponding to one slab part. The forces on each part were dependent on their geometrical dimensions and the hydrostatic pressure acting on them. The resultant of the hydrostatic load on each part was computed by considering them as a combination of prisms and pyramids. In this way, the center of gravity of each load can be obtained as shown in Figure 3. This procedure, however, requires the solution of highly nonlinear equations. Even for the special case where the support conditions were the same on AD and BC, which means $\varphi_1=\varphi_3$ and $\beta_1=\beta_2$, it is necessary to solve three equations. Since the analytical solutions were difficult, it was preferable to use numerical techniques and to solve the problem iteratively.

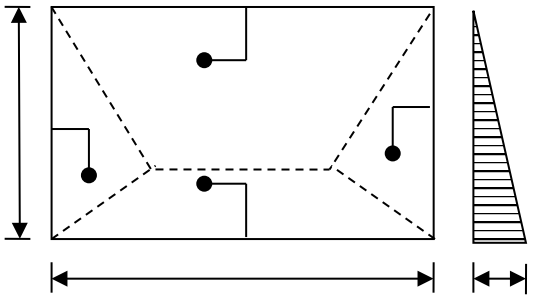

Figure 3. The center of gravity of load on each slabs part.

The algoritm presented here predicts the initial values for α,β_1, and β_2. Using these values the hydrostatic loads P_1, P_2, P_3, and P_4 acting on each slab part and their application points G_1, G_2, G_3, and G_4, as shown in Figure 3 were calculated [8,10]. In this case, the equilibrium equations become:

$$P_1 d_1 = mH + \varphi_1 mH = mH(1+\varphi_1) \quad (2)$$

$$P_2 d_2 = mb(1+\varphi_2) \quad (3)$$

$$P_3 d_3 = mH(1+\varphi_3) \quad (4)$$

$$P_4 d_4 = mb(1+\varphi_4) \quad (5)$$

where d_i is distance from centroid of i^{th} slab part to the side (see Figure 3), is vertical side lenght and b is horizontal side lenght.

The only unknown in the above equations is m. Obtaining the same value for m from each equation shows that the initial values of α,β_1, and β_2 were correct. Otherwise, it becomes necessary to repeat the above computation until the values of m obtained from each equation were equal to each other. In the case where the slab has one edge free, the solution becomes easier. It should be noted that the nodal forces were zero at the intersection of three positive yield lines.

3.2. Various support conditions

3.2.1. Slabs with three edges supported and one edge free

a) Case I:b>H (Figure 4)
In this case, consideration of the equilibrium equations for only slab parts 1 and 2 is sufficient. Carrying out the procedure explained above, the following equations are obtained:

$$m=\frac{\beta^2 b^2 \gamma H^3}{24[H^2(1+\varphi_1)-\beta^2 b^2]} \tag{6}$$

$$m=\frac{(1-\beta)H^3\gamma}{6(\beta+\varphi_2)} \tag{7}$$

In these equations nodal forces K_I and K_J($K_I = K_J = m\beta b/H$), on the nodal points I and J are also considered.Because of equilibrium these should be equal to each other. Hence,

$$\frac{\beta^2 b^2 \gamma H^3}{24[H^2(1+\varphi_1)-\beta^2 b^2]}=\frac{(1-\beta)H^3\gamma}{6(\beta+\varphi_2)} \tag{8}$$

β computed from Eq.(8), is substituted into Eq.(6) or Eq. (7) to obtain the value of ultimate bending moment per length.

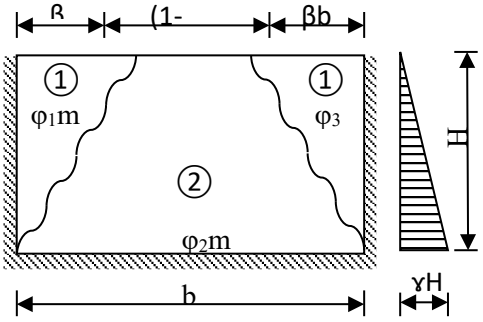

Figure 4. Slabs with three edges supported and one long edge free.

b) Case II: b<H (Figure 5)
In this case three yield lines occur at collapse as is shown in Figure 5. Considering the equilibrium equations for slab parts 1 and 2, it follows:

$$m=\frac{b^2\gamma H(9\alpha^2+2\alpha+1)}{96(1+\varphi_1)} \tag{9}$$

$$m=\frac{(1-\alpha)^2(1+\alpha)H^3\gamma}{12(1+\varphi^2)} \tag{10}$$

Since both Eqs.(9 and 10) should yield the same value of m, hence:

$$\frac{b^2\gamma H(9\alpha^2+2\alpha+1)}{96(1+\varphi_1)}=\frac{(1-\alpha)^2(1+\alpha)H^3\gamma}{12(1+\varphi^2)} \tag{11}$$

The ultimate moment per unit length is obtained by substituting the value of α which is found of from Eq. (11) into Eq. (9) or Eq.(10).

It should be noted that for b=H, the yield lines may be similar to or different from any given above.

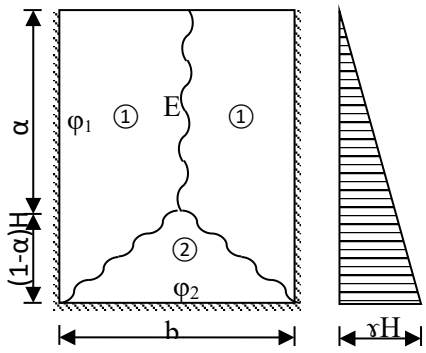

Figure 5. Slabs with three edges supported and one short edge free.

3.2.2 Slabs with all edges supported

a) Case I: Each edge having a different support condition (Figure 6).
In this case equilibrium equations are written for slab parts 1, 2, 3 and 4, which yields:

$$m=\frac{\beta_1^2 b^2 H\gamma(2\alpha+1)}{24(1+\varphi_1)} \quad (12)$$

$$m=\frac{H^3(1-\alpha)^2\gamma[-3\beta_1\alpha-3\beta_2\alpha-\beta_1-\beta_2+4\alpha+2]}{12(1+\varphi_2)} \quad (13)$$

$$m=\frac{\beta_2^2 b^2 H\gamma(2\alpha+1)}{24(1+\varphi_3)} \quad (14)$$

$$m=\frac{\alpha^3 H^3\gamma[4-3(\beta_1+\beta_2)]}{12(1+\varphi_4)} \quad (15)$$

It was apparent that the equations obtained are highly nonlinear. Hence, it was more suitable to employ numerical technique in their solution.

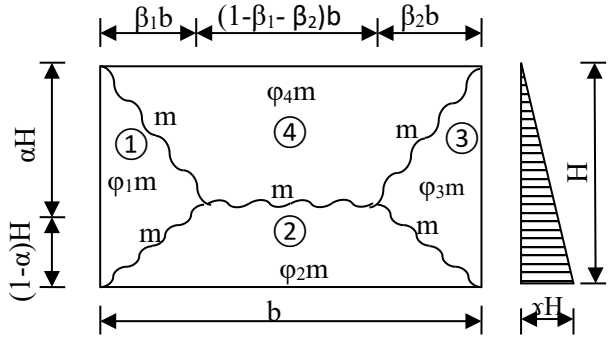

Figure 6. Slabs with each edge having different support condition

b) Case II: Corresponding edges having the same support conditions (Figure 7).
In this case slab parts 1 and 3 were identical. It becomes sufficient to substitute $\beta_1 = \beta_2 = \beta$ and $\varphi_1 = \varphi_3$ in Eqs. (12,13 and 15). After carrying out the simplifications the expressions for the bending moment per unit length for slab parts 1,2, and 3 become:

$$m=\frac{\beta^2 b^2 H\gamma(3\alpha^2+4(1-\alpha)\alpha+(1-\alpha)^2)}{24(1+\varphi_1)} \quad (16)$$

$$m=\frac{H^3(1-\alpha)^2\gamma[2\beta\alpha+(1-\alpha)\beta+(1-2\beta)\alpha+(1-\alpha)(1-2\beta)]}{6(1+\varphi_2)} \quad (17)$$

$$m=\frac{\alpha^3 H^3\gamma[\beta+2(1-2\beta)]}{6(1+\varphi_4)} \quad (18)$$

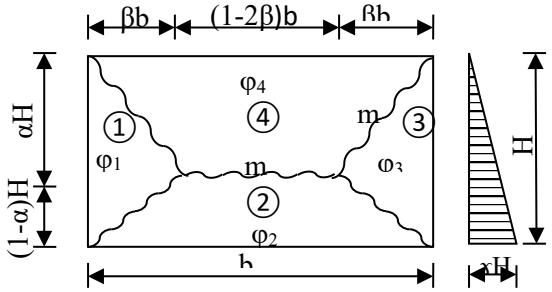

Figure 7. Corresponding edges having the same support conditions

The solution of the above nonlinear equations was carried out using an iterative technique. Calculated values (α and β) from above equations for different edge conditions are given in Table 1. It was apparent that such tables makes it possible to carry out the design of reinforced concrete slabs, such as tank walls, subjected to hydrostatic loading manually..

Table 1. α and β values according to edge ratio of all edges supported slabs with same support conditions of vertical edge

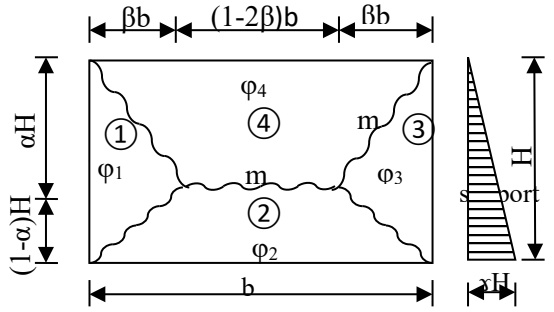

B/H	φ1= φ2= φ3=1		φ1= φ2=0,5 ; φ3=0		φ1=1 ; φ2= φ3=0		φ1= φ2= φ3=0	
	α	β	α	β	α	β	α	β
1,00	0,613	0,481	(*)	(*)	(*)	(*)	0,613	0,481
1,25	0,604	0,428	0,564	0,454	(*)	(*)	0,604	0,428
1,50	0,598	0,383	0,557	0,410	0,610	0,467	0,598	0,383
1,75	0,594	0,347	0,552	0,372	0,604	0,430	0,594	0,347
2,00	0,592	0,316	0,550	0,340	0,600	0,398	0,592	0,316
2,25	0,530	0,290	0,547	0,313	0,596	0,370	0,590	0,290
2,50	0,588	0,268	0,545	0,290	0,594	0,344	0,588	0,268
2,75	0,587	0,248	0,544	0,270	0,592	0,322	0,587	0,248
3,00	0,586	0,232	0,542	0,252	0,591	0,303	0,586	0,232

(*) Collapse mechanism is different

4. Conclusions

The developed equations based on yield line theory were presented for the design of reinforced concrete slabs which were supported along four sides and subjected to hydrostatic pressure. It was shown that the analytical computation of the ultimate moment per unit lenght requires the solution of a highly nonlinear system of equations. This difficulty was overcome by utilizing an iterative technique by computer program. It also gives the value of the ultimate moment per unit length of the yield line. The developed equations makes it possible to prepare tables that contain the values of parameters related to yield lines according to various support conditions and the ratio of slab edge lenghts. This in turn makes the design easy to be carried out manually for practical purposes. As a result, manual design of such slaws can be significantly simplified by the use of coefficient obtained by using the computer.

Conflicts of Interest

The authors declare no conflict of interest.

References

[1] Hüsem M.; Durmuş A. (1994). The Structural Analysis of Rectangular Water Tanks Using Different Method, Proceeding of the Second International Conference in Civil Engineering on Computer Applications, Research and Practice, University of Bahrain, pp. 241-251.

[2] Ferguson, P.M.; Breen, J.E.; Jirsa. J.O. (1998) Reinforced Concrete Fundamentals, 5th ed.; John Willy & Sons.

[3] Ghali, A.; Neville. A.M. (1996). Structural Analysis: A Unified Classical and Matrix Approach, 7th ed.; Ankara University Printing House, Ankara, Turkey.

[4] Hognestad, E. (1953). Yield-Line Theory for Ultimate Flextural Strength of Reinforced Concrete Slabs. *American Concrete Institute, 49*, 637-656.

[5] Johansen, K.W. (1962). Yield-Line Theory; Cement and Concrete Association, London.

[6] Johansen, K.W. (1972). Yield-Line Formulae for Slabs; CRC Press, Boca Raton.

[7] Johansen, K.W. (1969). Yield-Line Analysis of Slabs Supported on Three Sides. *American Concrete Institute, 66*, 741-744.

[8] Jones, L.L.; Wood, R.H. (1967). Yield–Line Analysis of Slabs; Thames & Hudson, London.

[9] Kong, F.K.; Evans, R.H. (2017). Reinforced and Prestressed Concrete; CRC Press, Boca Raton.

[10] Kvviecinski, M.W. (1965) Yield Criterion for initially isotropic reinforced slab. *Magazine of Concrete Research, 17*, 51.

[11] Massonnet. C. (1966). Théorie Générale des Plaques Elasto-Plastiques; International Association of Bridge and Structural Engineering Publication, Zurich.

[12] Meyer, C. (1996) Design of Concrete Structures, Prentice Hall, New Jersey.

[13] Morley, A.T. (1965). Special Publication on Recent Developments in Yield-Line Theory. *Magazine of Concrete Research, 19*, 211-222. https://doi.org/10.1680/macr.1967.19.61.211.

[14] Navy, E.G. (1996). Reinforced Concrete a Fundamental Approach, 3rd ed; Practice Hall, New Jersey.

[15] Shariati, M.; Rafie, S.; Mehrabi, P.; Zandi, Y.; Fooladvand, R.; Gharehaghaj, B.; Shariat, A.; Trung, N.T.; Salih, M.N.A., Poi-Ngian, S. (2019). Experimental investigation on the effect of cementitious materials on fresh and mechanical properties of self-consolidating concrete. *Advances in Concrete Construction, 8,* 225–237. http://dx.doi.org/10.12989/acc.2019.8.3.225.

[16] Zanadi Y.; Akpinar, M.V. (2012). An experimental study on separately ground and together grinding Portland slag cement strength properties. *Research Journal of Recent Science, 1*, 27–40.

[17] Zandi, Y.; Akpinar, M.V. (2012). Evaluation of internal resistance in asphalt concretes. *International Journal of Concrete Structures and Materials, 6,* 247–250. http://dx.doi.org/10.1007/s40069-012-0021-0.

[18] Shariati, M.; Heiati, A.; Zandi, Y.; Laka, H.; Toghroli, A.; Kianmehr, P.; Safa, M.; Salih, M.N. A.; Poi-Ngian, S. (2019). Application of waste tire rubber aggregate in porous concrete. *Smart Structures and Systems, 24*, 553–566. https://doi.org/10.12989/sss.2019.24.4.553.

[19] Nosrati, A.; Zandi, Y.; Shariati, M.; Khademi, K.; Aliabad, M.D.; Marto, A.; Mu'azu, M.A.; Ghanbari, E.; Mahdizadeh, M.B.; Shariati A.; Khorami, M. (2018). Portland cement structure and its major oxides and fineness. *Smart Structures and System, 22*, 425–432. https://doi.org/10.12989/sss.2018.22.4.425.

[20] Zandi, Y.; Burnaz, O.; Durmus, A. (2012). Determining the temperature distributions of fire exposed reinforced concrete cross sections with different methods. *Research Journal of Environmental and Earth Sciences, 4,* 782-788.

[21] Zandi, Y.; Alayi, M (2019). Effect of comparison of Ardabil pozzuoli cement and type 2 Sufyan cement compressive strength viewpoints and improvement solutions. *Journal of Structural and Construction Engineering, 6*, 95–110. https://dx.doi.org/10.22065/jsce.2018.117984.1454.

[22] Zandi, Y. (2013) Effect of mix design on restrained shrinkage of concrete. *Bulletin of Environment and Life Sciences, 2*, 13–20.